Proceedings of the ASME 2015 International Mechanical Engineering Congress and Exposition
IMECE2015
November 13-19, 2015, Houston, Texas

IMECE2015-52045

USING LES TO UNDERSTAND WAKE EVOLUTION DURING THE DIURNAL CYCLE

Jordan Nielson
Graduate student, Department of Mechanical Engineering, University of Texas, San Antonio, TX, USA, 78248
Email: mmr315@my.utsa.edu,

Kiran Bhaganagar
Associate Professor, Department of Mechanical Engineering, 1 UTSA Boulevard, San Antonio, Texas, 78248 Email: Kiran.bhaganagar@utsa.edu, Telephone: 210-458-6496

ABSTRACT

Numerical study using actuator-line method based Large Eddy Simulation (LES) has been performed to understand the role of atmospheric stability on the wake effects of horizontal-axis full-scale 5-MW wind turbine (WT). The paper will specifically focus on using specific instances in the diurnal cycle corresponding to stable, neutral and unstable ABL state to gain understanding on the transient aerodynamics of a wind turbine throughout the diurnal cycle. Capturing accurate Atmospheric Boundary Layer (ABL) characteristics is key factor in improving the accuracy of WT model predictions as turbulence developed in the ABL has potential to adversely affect the fatigue lifetime and performance of wind turbines. ABL simulations for the diurnal cycle are performed to isolate the key ABL metrics such as surface momentum flux, boundary layer height, surface temperature flux, wind shear, and temperature gradient that influence the wake evolution of WT. Precursor ABL inflow is generated for the WT simulations. The positive heat flux on the surface causes high vertical velocity fluctuations described with streaks and updraft motions during the day while surface cooling rates result in increased shear and strong temperature gradients during the night. The surface temperature, geostrophic wind velocity, heating/cooling rates, and period of the diurnal cycle are varied in different simulations to compare turbulent statistics and the helical vortices of the wind turbine wake. The results have revealed surface temperature and surface flux are the important ABL metrics that have a strong effect on altering the turbulence in the WT wake. In addition, instabilities related to WT blade rotation exhibit sensitivity to ABL metrics. The positive heat flux shows higher mixing and causes large wake movement in the day-time conditions. The results aid in quantifying the movement of the wake at different times of the diurnal cycle. During night-time conditions mixing is low, causing slower wake recovery times. This is the first study to clearly isolate the key ABL metrics that influence the full-scale WT near-wake effects The study has implications in improving the predictions of WT power loss due to wake deficits. Further, this study sets an important direction on future modeling studies in identifying the ABL conditions in a diurnal cycle that influence the WT wake evolution.

INTRODUCTION

Full-scale WT operate in atmospheric boundary layers, which is a part of the atmosphere that interacts with the earth. The State of Atmospheric boundary layer (ABL) significantly influence the wake generated by the WT, in particular, the differences in the turbulent kinetic energy (TKE), competing roles of TKE production mechanisms, namely, wind shear vs. thermal buoyancy production, wind shear and temperature gradients. . However, to-date, most of the numerical studies are based on idealistic flow conditions and do not account for ABL effects. Further, to simulate all the instances of a diurnal cycle is computationally intensive. What is urgently needed is to understand the key physics of the ABL and the differences that arise due to atmospheric stability. For this purpose, we need to identify the metrics of the ABL state during different stability conditions, namely, stable, unstable or convective and neutral state. Recent work [1, 2] has clearly suggested response of wind turbine wake evolution is

significantly linked to ABL conditions. Bhaganagar & Debnath [3] have established wind shear and vertical thermal gradient dictate the TKE in the WT wake region of operation in stable ABL. The motivation of the present study is to

1. to isolate the key ABL metrics that impact the wake physics of WT operating under unstable and neutral stability conditions,
2. demonstrate the significance of realistic ABL inflow conditions for WT simulations,
3. And to identify the additional metrics that play a role compared to the WT in a stable ABL state.

One of the key forcing mechanisms of the ABL is heat transfer to/from the ground. The ABL is divided into convective, stable, and neutral states determined by potential temperature which is driven by surface heat transfer. Convective ABL occurs during the day as radiation from the sun heats the surface of the earth. As the surface heats, so does the air near the surface. The warm air rises until it heats a capping inversion where it cools and drops. The large movement of air creates mixing in the ABL. The daytime mixing allows for an almost uniform velocity profile except for the shear due to the friction of the surface [5]. The nighttime profiles differ greatly from those during the day. The surface begins to cool during the night causing negative buoyancy flux which dampens turbulence and lowers the Capping inversion. This causes the wind velocity to have a strong gradient, and can even produce lower level jets (wind speeds higher than geostrophic) [4]. Wind shear has been determined as a factor that causes error in power curve estimation [6] and also increases the amount of turbulence. In between the Stable and Convective ABLs, is a state when there is no surface flux called neutral. The temperature does not play an active role in the neutral state. Strong diurnal effects from surface heat flux cause land based wind farms to experience significant variations in the wind (strong winds during night-time or winter months and lower speed winds during day-time or summer months) and temperature conditions (the temperature gradient is positive during the night and negative during the day). Wind shear and temperature gradients have a strong effect on the amount of turbulence produced. A strong temperature gradient in nighttime conditions can aid in WT wake recovery [1].

The Convective ABL has strong mixing and a high boundary layer height leading to strong turbulence. The turbulence is much larger than for stable and neutral conditions. Turbulence is particularly important ABL metric of focus in wind energy as high turbulence has been shown to cause under-prediction of the power curve [6] and has also been shown to impact fatigue loading/reliability, maintenance, and life spans of wind turbines [2]. The turbulence in the Convective ABL can have negative impacts on the fatigue lifetime and performance of wind turbines, creating the importance for correctly simulating the ABL. Rather than simulating the WT effects with a given wind profile, in this study realistic ABL conditions are being generated to represent the inflow and initial conditions, For this purpose, quasi-equilibrium ABL solution is generated numerically for a given surface conditions. The precursor ABL simulation is simulated for a period long enough to reach quasi-equilibrium. The obtained quasi-equilibrium solution is then used as initial conditions for the WT simulations, thus representing real-life ABL conditions for the given stability state of the atmosphere. Many works show improved predictions of wake effects from realistic atmospheric inflow over inputting turbulence at the inflow [1, 2].

Convective, neutral and stable states of the atmosphere influence the instability mechanisms in the near-wake region, which include, wake meandering, wake tip-vortex interactions and helical vortex instability. Wake meandering is a process where the wake of the wind turbine moves vertically and/or horizontally in respect to the original position of the wind turbine [7]. Wake meandering causes fluctuations in power production and wind turbine loading of downwind turbines. Vortex instability includes mutual inductance between two consecutive rings of the helical vortex behind the wind turbine [8]. The two vortices will merge. The effects of these instabilities on Wind Turbines are not completely understood.

The realistic atmospheric flow better captures ABL metrics that occur in nature. The objective of the present work is to generate realistic ABL conditions for different atmospheric stability states and to isolate the key ABL metrics for each of these stability states. Further, the consequences of the differences in key ABL metrics for WT operating in unstable and neutral conditions are discussed.

METHODOLOGY

Large eddy simulation methodology was used in this study. We used the OpenFoam based Simulator for Offshore Wind Farm Applications (SOWFA). OpenFoam is a modular code design open source CFD software package [9]. In SOWFA 3-D incompressible Navier-Stokes equations are solved using the Boussinesq equation [9]. SOWFA tool was also used to generate real atmospheric flow. An initial heat flux, surface temperature, capping inversion height, and geostrophic velocity are prescribed as initial conditions. Temperature perturbations are used to initiate turbulence in the ABL simulation, which is simulated until it reaches a quasi-equilibrium state. We simulated two cases for the study, convective and neutral. As described supra, the major difference in the simulations is the heat flux at the surface. The first study simulated a moderately convective ABL with a surface temperature flux of 0.04 Km/s [10]. The second simulation simulated a neutral ABL with no temperature flux. For both simulations a 3 km x 3km x 2km boundary was used with Periodic boundary conditions on the N, S, E, and W faces. The simulations were performed with a 10m resolution. Both simulations used a 300 K initial surface temperature with the geostrophic velocity near 12.5 m/s. The

initial wind direction was set to be 225° (with 270° being east). The simulation represents 45°N latitude in summer conditions. The capping layer boundary was determined using the Gaussian distributions from Liu [14]. The convective ABL had a capping inversion height of 860m while the neutral ABL had a capping inversion height of 600. The two ABLs were compared to identify ABL metrics that would better improve prediction of wind Turbine operation. For the paper, the convective ABL will be referred to as CABL while the neutral ABL will be referred to as NABL (there definitions can be seen in the Introduction). After the ABL flow was fully developed (momentum flux and heat flux reached quasi-equilibrium), statistics were averaged for 30 minutes.

After the precursor ABL was generated, we used the Actuator Line Model (ALM) to approximate the rotor of the WT. The WT simulated is an NREL 5MW wind turbine with a hub height of 90m and a diameter of 126m. For ALM, the body forces of the blade are estimated using the rotor's airfoil data. These body forces are applied radially on a line using a Gaussian distribution. We used a Gaussian width of twice the grid size to smoothly capture the forces of the rotor. Using the ALM method, we were able to represent the rotor with 50 radial points per blade.

For the WT simulations, we created a boundary the same size and resolution as the original (3 km x 3km x 2km boundary with a 10m resolution). We then refined the mesh to 1.25m resolution in the area of the Wind Turbine and in the near wake. The ABL simulations are mapped to the refined boundary and are run by passing the simulated ABL through the Wind Turbine.

It should be noted that for the ABL results the *x* direction is east, while for the WT results the *x* direction is in the stream wise wind direction.

RESULTS: ABL SIMULATIONS

The flow characteristics for the velocity profile and temperature profile are shown in Figure 1. The figure shows the complete ABL profile, as well as a zoomed in profile with a scale representation of the WT. The temperature profile clearly shows the capping inversion layers for the two simulations remained relatively constant at 860m for the CABL and 600m for NABL during the simulation. The heat flux in CABL causes the surface temperature to rise almost 1 K near the surface shown in FIG. More importantly, the heat flux causes a temperature gradient to around 200m, well above the upper tip of the 5MW turbine. The temperature gradient of the CABL creates the buoyancy effects that generate mixing. The mixing can be seen in the velocity profiles. The velocity profile for the CABL shows the sharp instability near the capping inversion layer. Near the capping inversion the velocity grows significantly to the geotropic velocity which is characteristic convective ABLs [11]. The instability causes a smaller wind shear with a near uniform wind speed for the CABL, even though both simulations have similar geostrophic wind velocities. FIG shows that even though the CABL is uniform for 70-80% of the ABL, the WT still sees a strong wind gradient, especially below the hub. For both simulations the wind angle increases slightly with height with changes of about 5° from the ground to the inversion height. The wind angle for the CABL and NABL remain much less than those found in the Stable ABL [1]. For both simulations the final wind direction at hub height was approximately 247°.

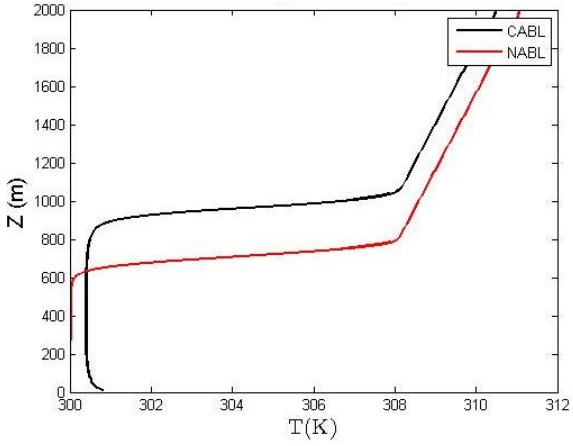

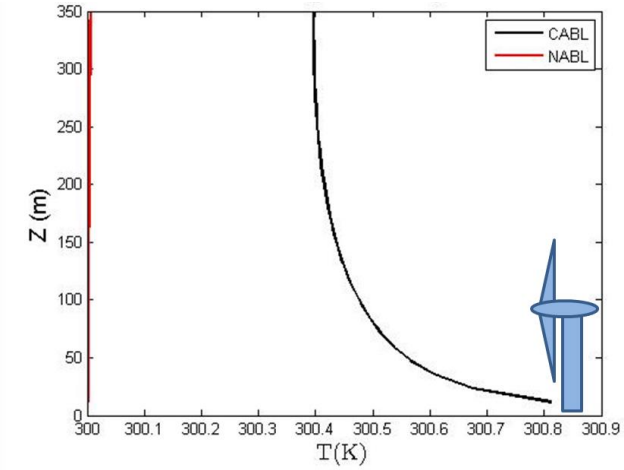

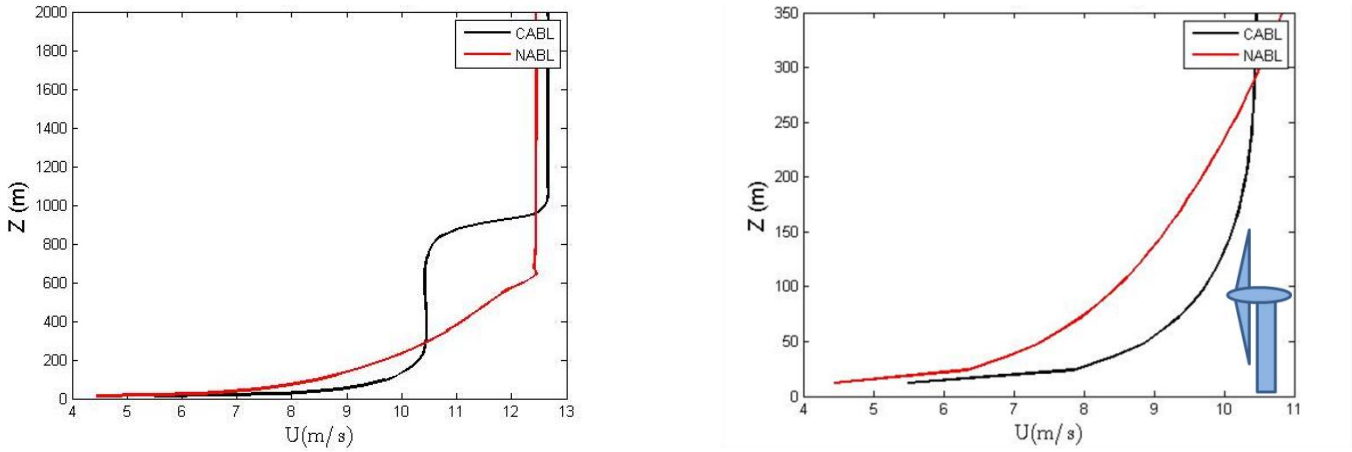

Figure 1: (a) NABL Wind velocity Profile, b) CABL Wind velocity Profile, c) NABL Temperature Profile, d) CABL Temperature Profile.

While power output is commonly determined by the hub height velocity, real wind turbines see a shear gradient across their faces which can cause over or underestimation of the power output [6]. Wind shear can be described with an exponent alpha based on equation 1[12].

$$\frac{u_i}{u_{hub}} = \frac{z_i}{z_{hub}}^{\alpha} \qquad \text{Eq. 1}$$

Alpha was found for both simulations by taking the average wind speed profile and comparing this to a profile generated by eq.1. The alpha value that minimized the root mean square between the real and the generated profile was accepted as the shear exponent of the simulation. The wind shear exponent was estimated to be 0.06 for CABL and 0.19 for NABL. Both values fell in the expected range from experiments [5]. Again, even though the shear exponent is much less for CABL, Figure 1d) shows wind shear still plays a large role below the hub.

The increased heat flux of the CABL also affects the Reynolds stresses. The Reynolds Stresses show the strength of the turbulent fluctuations stresses and represents the momentum transport by turbulent convection. The Reynolds Stresses were broken down into *u'u'*, *v'v'*, and *w'w'* components and are shown in Figure 3. The Reynolds's stresses for CABL were about 80% higher than NABL near the surface and stay much higher the entire height of the WT. For both cases the *u'u'* and *v'v'* Reynolds Stress Profiles are similar, but the CABL had a sharp increase near the inversion layer due to the instability. The vertical Reynolds stress *w'w'* differs greatly between the two cases. The CABL *w'w'* Reynolds stress does not start to decrease until well past 250m [13], which is well above the height of the 5MW wind turbine. The heat flux greatly increases the amount of turbulent fluctuations in the vertical direction which aids in the mixing described supra. The CABL Reynolds stress profiles closely matched those calculated for a 0.04 Km/s heat flux [10]. The Reynolds stresses are also used to estimate the boundary layer height both ABL profiles. The value is calculated as 1/0.95 of the value when *u'w'* falls below %5 of the surface value. The boundary height for the CABL is estimated to be 900m, while the boundary layer height of the NABL is estimated at 600m [14]. Both of the boundary heights are well above the region of the WT (upper tip is 153m), which is very different from the boundary layer height found in Stable ABL [1, 4]. As a result the boundary height is not expected to greatly affect the WT aerodynamics for the CABL and NABL cases.

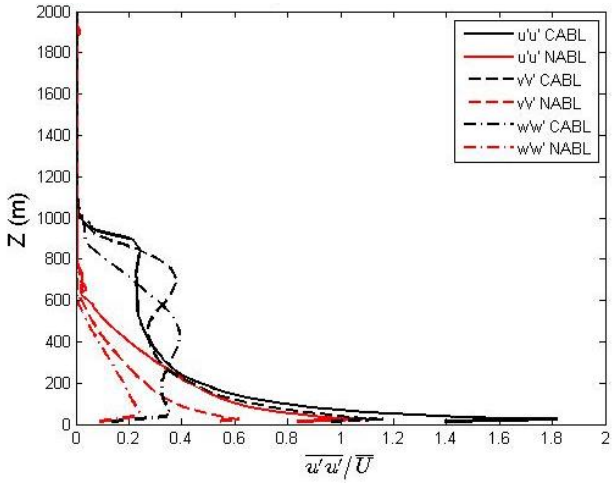

Figure 2: NABL and CABL Reynolds Stresses.

In addition to looking at the Reynolds stress averaged profiles, we looked at the *w'w'* structures. The *w'w'* structures are shown at the WT hub height (90m) in Figure 3. At 90m the vertical Reynolds stress for the CABL has distinct "updraft" structures separated in the spanwise direction which are described well by Mason [15]. The updraft motions appear as air is heated by the warm surface as described in the

introduction. The updraft features are aligned with the wind direction spread further apart as height increases. Eventually the features disappear as they penetrate the inversion layer. The NABL vertical Reynolds stresses appear in more random form. In addition the growth in Reynolds stress from 90m to 150m was double for the CABL. Unlike the stable ABL, these vertical structures are present through the height of the Wind Turbine [1]. The vertical structures aid in the mixing of the CABL.

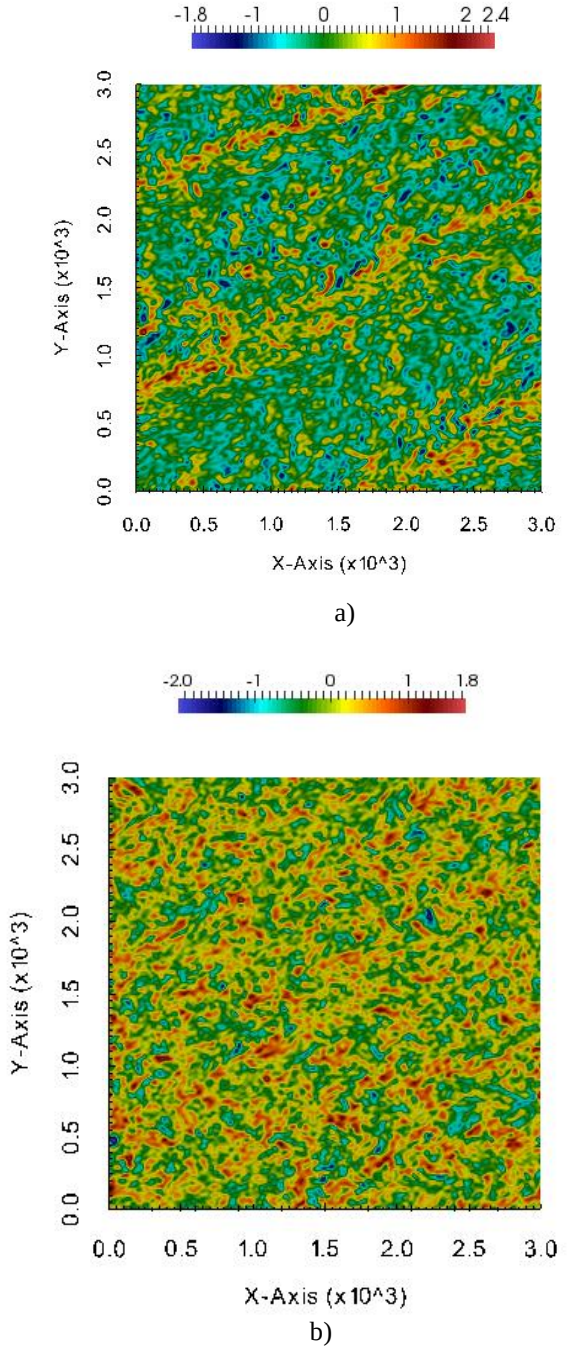

Figure 3: a) CABL w'w' at Hub Height, b) NABL w'w' at Hub Height.

The velocity profiles can be combined with the turbulent statistics using Eq.2 and Eq.3 to get the buoyancy and shear production terms respectively.

$$\overline{w'T'} \qquad \text{Eq. 2}$$

$$\overline{u'w'}\frac{d\bar{u}}{dz} - \overline{v'w'}\frac{d\bar{v}}{dz} \qquad \text{Eq.3}$$

Although the shear exponent is higher for the NABL, the near homogenous velocity profile for CABL forces the wind shear to be greater near the surface. The CABL shear production is therefore larger until 90m height. The CABL shear production then approaches zero quickly while the NABL shear production continues to the inversion layer. The CABL simulation has buoyancy production near the surface and at the inversion layer. The NABL does not have buoyancy production (due to constant T). The CABL WT will see much larger shear and buoyancy production below the hub height. The combination of the high shear and buoyancy production near the surface of the CABL causes strong mixing and turbulence.

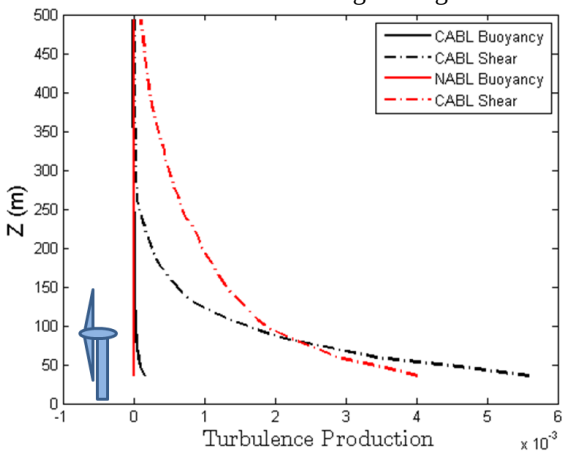

Figure 4: Turbulence Production.

The velocity profile and temperature profiles can also be used to calculate the Richardson Number. The Richardson number is a metric for Stability, found from the ratio of the buoyancy and flow gradient. The Richardson Number is calculated in Eq. 4.

$$R_i = \frac{\frac{g}{\overline{\theta_v}}\frac{\partial \theta_v}{\partial z}}{\frac{\partial \bar{U}^2}{\partial z}} \qquad \text{Eq. 4}$$

The Richardson number was calculated to be approximately 0 for NABL and -0.09 for the CABL following experimental results. The Richardson number has been used to determine if the effects of gravity will suppress turbulence. The Richardson number aids in determining how turbulence in wind turbines is suppressed.

The Reynolds stresses are also used to measure turbulence using turbulent kinetic energy (TKE) or turbulence intensity [5]. Eq. 5 shows how the TKE is calculated.

$$\frac{1}{2}\left(\overline{u'u'} + \overline{v'v'} + \overline{w'w'}\right) \qquad \text{Eq. 5}$$

CABL has both shear and buoyancy production producing about 25% more TKE than the NABL at hub height. The TKE shows an increase near the inversion layer due to the instability. The turbulence intensity of 12% at hub height for the CABL and 9% for the NABL follow close to the data measured in field experiments [5]. The mixing in the CABL causes the turbulence to remain relatively homogenous from 400-800m before it hits the inversion layer.

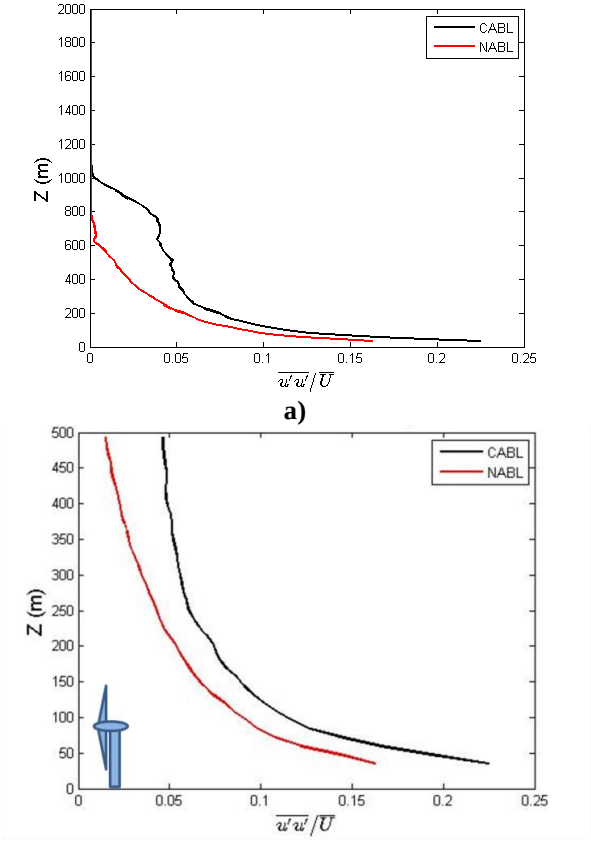

Figure 5: Turbulence Intensity a) Complete Profile, b) With WT for reference.

DISCUSSION: ABL SIMULATIONS

The stability of the atmosphere is altered by changing the surface heat flux. Stability of the ABL significantly alters the ABL flow dynamics that influence the WT wake development. The major differences between the CABL and NABL simulations are summarized in Table 1. Under unstable ABL conditions, TKE is generated both by the shear production and buoyancy production resulting in a higher TKE, thus resulting in increased mixing in the ABL and forming a well-mixed boundary layer. The mixing was seen in the vertical Reynolds stress. The CABL has a distinct pattern of "updrafts" and "downdrafts" making up the convective rolls. The pattern is also seen in the magnitude of the Reynolds stresses, where streaks aligned with the wind direction, can have 4x the magnitude of turbulence. The CABL also has an increase in the *w'w' vertical* Reynolds's stress component between 100m-400m, which is a strong difference in the area of the wind turbine.

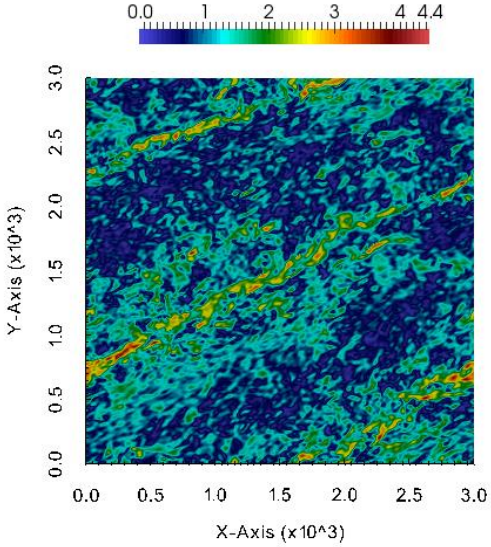

Figure 6: CABL Reynolds Stress Magnitude.

Table 1: Results of Simulations

Simulation	q (Km/s)	Ri	α	Turbulence Intensity (Hub Height)	Reynolds Stresses	Boundary Height	U (m/s) Hub Height	dT/dz (K/m)	Buoyancy Production	Shear Production
CABL	0.04	-0.09	0.06	12%	Coherent Streaks	900m	9.6	-.002	Near Surface	Near Surface
NABL	0.00	0.00	0.19	9%	Random	600m	8.3	0.0	None	Through Boundary

RESULTS: WIND TURBINE

After generating the precursor ABL state, WT simulations are performed using the Actuator Line Method [16]. The ALM simulations performed in this paper do not include the effects of the hub or tower, but only the blades. To begin we look at the Power generated by the WT in the two ABL states. The CABL simulation produced 180% more power than the NABL wind turbine. This is expected as Figure 1d) shows that the WT sees greater velocities at every point across the blade diameter. The power is often estimated by using the cube of the velocity at hub height. Using this method we would expect the CABL to increase the power 155% more than NABL. The simulation predicts higher gains in power production between the two because it accounts for the difference in wind speed at every point of the diameter rather than just from the hub. To better understand the effects of shear on wind production it would be appropriate to perform precursor Neutral and Convective ABLs with the same hub height, which is outside the scope of this paper.

The TKE in the wake of the wind turbine at Y=0 are shown in Fig.7. The magnitude of the CABL TKE is about 25% higher than NABL. The biggest difference between the NABL and CABL cases is the upper tip. The NABL case for the upper tip slowly grows in width beginning at 1D. This growth is expected to be caused by the shear production that occurs above the hub height. The TKE from the upper tip eventually gets wide enough that it interacts with the hub TKE. The upper tip for the CABL case is much more concentrated. Although it hits the higher value, it does not have a large growth in width and begins to die around 3-4D. The CABL TKE profile at the lower tip grows in width more than the NABL profile. The NABL lower tip TKE starts to recover by 2D. The CABL lower tip TKE does not begin to recover until 5D. The different TKE profiles will have large affects on the loadings of WT downstream as the NABL profile might require extra distance for the TKE to recover the Upper tip TKE.

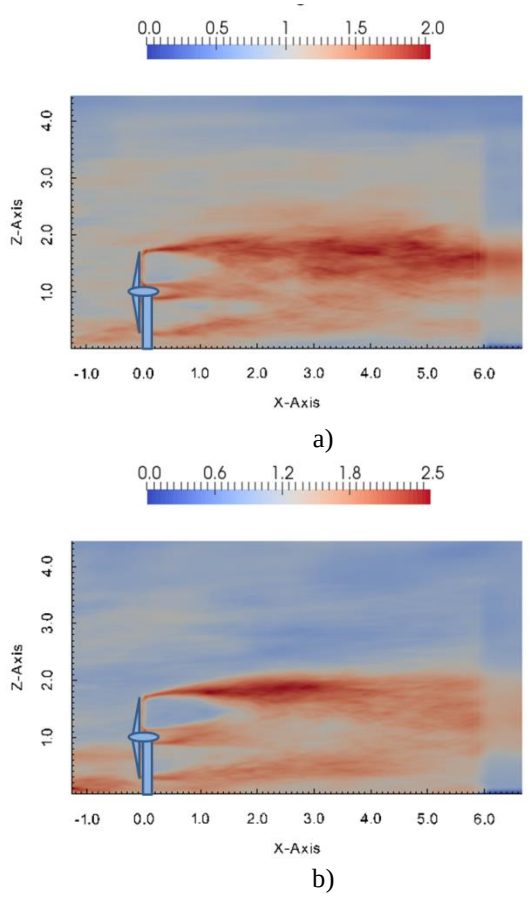

Figure 7: TKE Profiles at Y=0 for a) NABL b) CABL.

Further, the wake deficits were plotted as shown in Figure 8. The wake deficits are greatly affected by the amounts of TKE in the wake. The CABL show much faster recovery below the hub. This comes from the larger amounts of TKE in this region due to buoyancy production and strong shear near the surface. The upper tip wake deficits are similar for the CABL and NABL simulations. Although the TKE was stronger for CABL at 2-3D, the NABL upper tip turbulence continues to grow past this point increasing wake recovery. Overall the CABL simulation recovers faster even though some points above the hub recover slower than NABL. The large amounts of TKE generated by the CABL inflow allow for mixing and cause a smaller wake deficit [17].

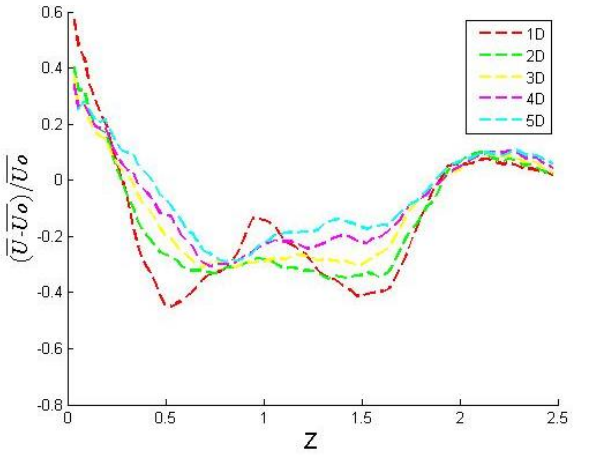

a)

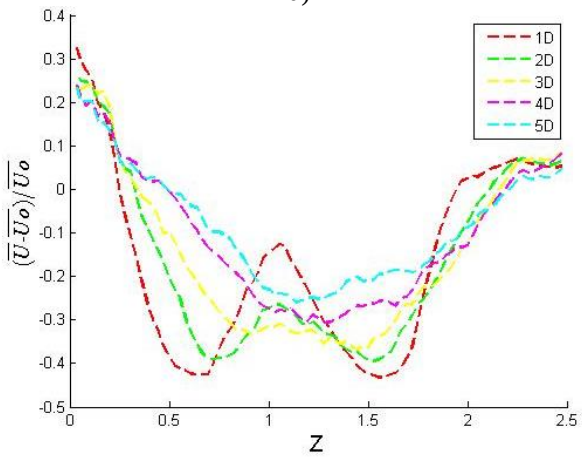

b)

Figure 8: 2D Wake Deficit Plots at Y=0 for a) NABL b) CABL.

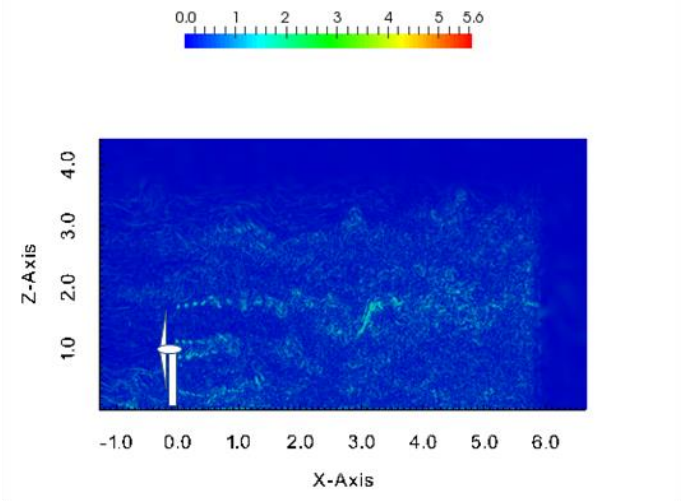

a)

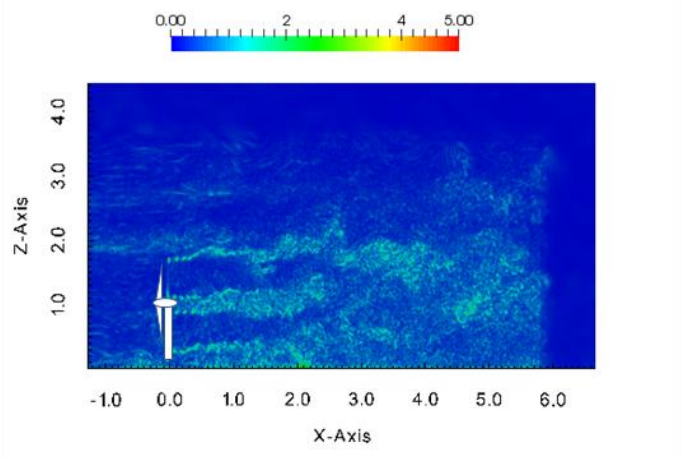

b)

Figure 9: Vorticity Structures at y=0D for a) NABL, b) CABL.

The NABL and CABL instantaneous vorticity structures are compared in Figure 9. The strong shear of the ABL causes the hub structure to dissipate near 1D. The result is that the structures from the upper tip and hub do not interact and the lower tip vortex advects upward between 1 and 2D. This phenomenon is more pronounced when the shear is even larger in some Stable ABL cases [3]. For the CABL, the strong mixing from the buoyancy forces results in the hub and upper tip structures to interact. Near 2D the hub structures begin to rise towards the upper tip. The CABL also shows characteristics of meandering in the x-z plane as the path of upper tip structures is not liner. This is different than the structure seen at 3D in the NABL that is merely a result of the shear layer. Although the effects of vorticty on WT are not completely understood, the CABL WT would have more vorticy interacting with WT downstream.

The further investigation of meandering of the CABL structures was performed by looking at the 3-D Coherent structures using Lambda2 criterion. The large amounts of turbulence caused the vortical spirals to break up near 1D. It was after this point, between 1D and 2D that the wake begins to meander. The meandering wake reaches a height nearly 15% higher than the original tip height. The coherent structures also show the high amounts of turbulence near the lower tip. The turbulence near the ground causes the lower tip vortical spirals to break before the upper tip vortical spirals.

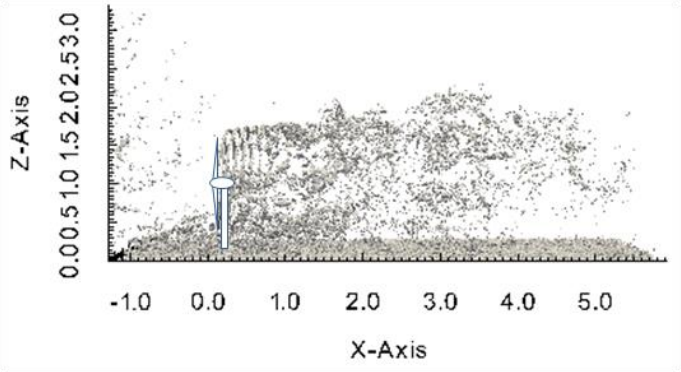

Figure 10: Lambda2 Structures for CABL.

The vorticity was also plotted at 4 different time instances for Y=0. The time difference between the snapshots was 9s. For all snapshots the upper tip, lower tip, and hub structures keep their shape relatively well for the first diameter. It was around 1D that the meandering of the structures begins. Figure 9b show mutual inductance between the 6th and 7th helical spiral on the upper tip similar to that found in experiments by Sorenson [7]. By separating the snapshots in time we can also see the growth of meandering over time. In Figure 9a at 0.75D we see the helical cores beginning to break up and rise vertically. The same structure can be seen in Figure 9b near 1.2D, but the structure has risen and the cores are no longer discernible. The structure raises even higher at 1.9D in Figure 9c and again even higher at 2.4D in Figure 9d. The time series plots show there is a correlation between time periods. Also, due to meandering, the wake expands as it travels.

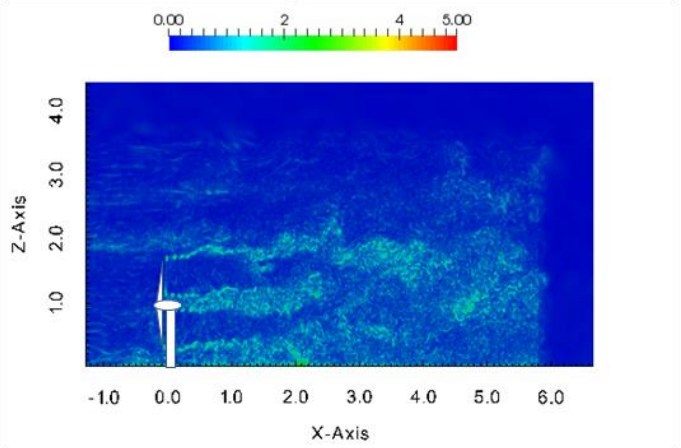

a)

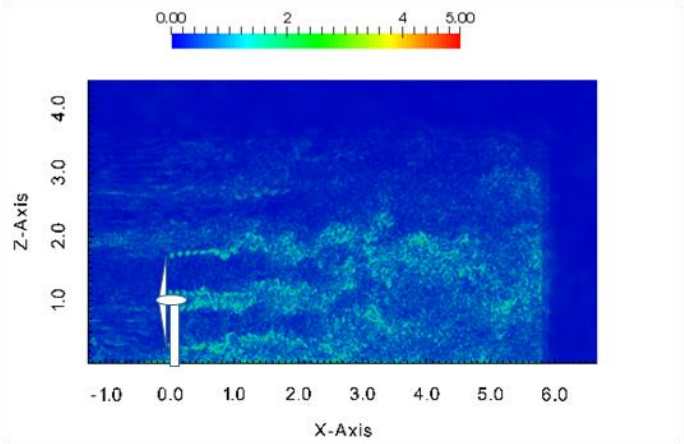

b)

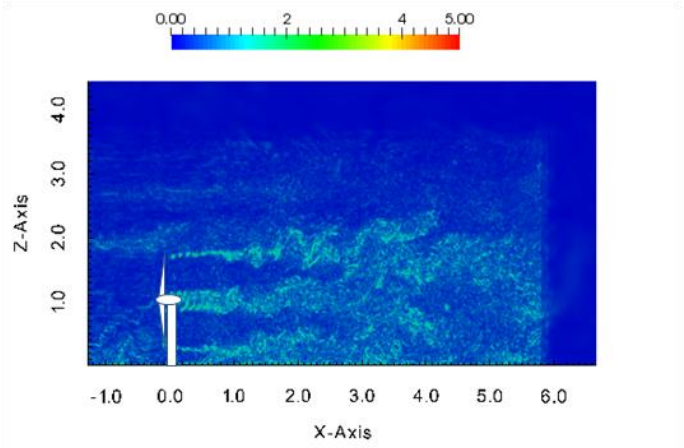

c)

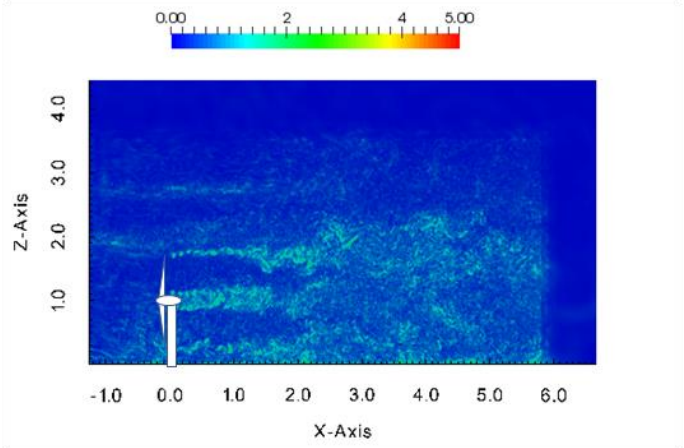

d)

Figure 11: Vorticy structures for CABL, a) 107s b) 116s c) 125s d) 134s.

CONCLUSION

In conclusion, we have isolated the Atmospheric Boundary Layer metrics that influence the wind turbine generation. Key metrics include surface flux, wind shear,

vertical turbulence flux *w'w'*, Turbulence Intensity, and shear/buoyancy production. Modeling the atmospheric boundary layer aided in the prediction of power generated over the diameter of the turbine. For the Convective and Neutral Atmospheric Boundary Layer height did not play a strong role in the wind turbine wake because the heights were well above the upper blade tip. This is not true for Stable cases as the boundary height lowers to a height between the upper and lower tips [3]. The *w'w'* structures and turbulence production add to the amount of turbulent kinetic energy experienced in the convective atmospheric boundary layer. The convective atmospheric boundary layer inflow caused an increase in turbulence seen by the wind turbine. But the shear and buoyancy affects altered the turbulence that would be seen by downstream wind turbines. Namely, the wind turbine in the neutral boundary layer showed a growth of turbulence at the upper tip not seen by the wind turbine in the convective boundary later. Therefore the shear and buoyancy production is important metric that influences the wind turbine wake evolution. Under convective stability conditions buoyancy and shear production enhance the total turbulence generated and thus result in uniform mixing and a faster wake recovery. However, due to the high turbulence, significant wake meandering and blade tip-vortex merging, these phenomena have greater effects on downstream wind turbines. The study clearly demonstrates the importance of realistic ABL initial and inflow conditions for accurate predict of wind turbine performance. Further, the present study sets a direction for the future Wind Turbine studies of using the Atmospheric Boundary Layer metrics to understand the wake-wake interactions in a wind farm during a diurnal cycle. The study is offered as a contribution to Wind Turbine wake physics and the significance of realistic Atmospheric Boundary Layer forcings.

ACKNOWLEDGMENTS

KB acknowledges the support from NSF Energy for Sustainability program under CBET-1348480. The authors acknowledge the Texas Advanced Computing Center (TACC) at The University of Texas at Austin for providing {HPC, visualization, database, or grid} resources that have contributed to the research results reported within this paper. URL: http://www.tacc.utexas.edu.

REFERENCES

[1] Bhaganagar, K., and Debnath, M., 2015, "The Effects of Mean Atmospheric Forcings of the Stable Atmospheric Boundary Layer on Wind Turbine Wake," AIP Journal of Renewable and Sustainable Energy., **7**, 013124. (doi: 10.1063/1.4907687).

[2] Mirocha, J. D., Kosovic, B., Aitken, M. L., Lundquist, J. K., 2014, "Implementation of a Generalized Actuator Disk Wind Turbine Model Into the Weather Research and Forecasting Model for Large-Eddy Simulation Applications," Journal of Sustainable and Renewable Energy, **6**, 013104. (doi: 10.1063/1.4861061).

[3]Bhaganagar, K., Debnath, M., 2014 "Implications of Stably Stratified Atmosheric Boundary Layer Turbulence on Near-Wake Structure of Wind Turbines," Energies, 7, 5740-5763; doi:10.3390/en7095740

[4] Basu, S., Porté-Agel, F., 2005, "Large-Eddy Simulation of Stably Stratified Atmospheric Boundary Layer Turbulence: A Scale-Dependent Dynamic Modeling Approach," St. Anthony Falls Laboratory, University of Minnesota.

[5] Wharton, S., Lundquist, J. K., 2012, "Atmospheric Stability Affects Wind Turbine Power Collection," Environmental Research Letters, **7**, pp. 1-9.

[6] Elliot, D. L., Cadogan, J. B., 1990 "Effects of Wind Shear And Turbulence on Wind Turbine Power Curves." CONF. 900989, *1990 European Community Wind Energy Conference and Exhibition* Richland, Washington, Pacific Northwest Laboratory

[7] Larsen, G.C., Madsen, H. A., Thomsen, K., Larsen, T. J., 2008, "Wake Meandering: A Pragmatic Approach," Wind Energy, **7**, pp. 377-395. (doi:10.1002/we.267).

[8] Sorensen, J. N., 2011, "Instaility of Helical Tip Vortices in Rotor Wakes," Journal of Fluid Mechanics, **682**, pp. 1-4.

[9] Lee, S., Churchfield, M., Jonkman, J., Michalakes, J., 2012 "Atmosheric and Wake Turbulence Impacts on Wind Turbine Fatigue Loadings" AIAA 2012-0540 *50th AIAA Aerospace Sciences Meeting including the New Horizons Forum and Aerospace Exposition 09 - 12 January 2012, Nashville, Tennessee*

[10] Moeng, C. H., Sullivan, P. P., 1993, "A Comparison of Shear- and Buoyancy-Driven Planetary Boundary Layer Flows," Journal of Atmospheric Sciences, **51** (7), pp. 999-1022.

[11] Tenners, H., 1973, "A Model for the Dynamics of the Inversion Above a Convective Boundary Layer," Journal of the Atmospheric Sciences, **30**, pp. 558-567.

[12] Wagner, R., Courtney, M., Gottschall, J., Lindelöw-Marsden, P., 2011, "Accounting for the Speed Shear in Wind Turbine Power Performance Measurement," Wind Energy. (doi: 10.1002/we.509)

[13] André, J. C., Moor, G. D., Lacarrère, G. T., Vachat, R. D., 1978, "Modeling the 24-Hour Evolution of the Mean and Turbulent Structures of the Planetary Boundary Layer," Journal of the Atmospheric Sciences, **35**, pp. 1861-1883.

[14] Liu, S., Xin-Zhong, L., 2010, "Observed Diurnal Cycle Climatology of Planetary Boundary Layer Height," Journal of Climate, **23**, pp. 5790-5809.

[15] Mason, P. J., 1988, "Large-Eddy Simulation of the Convection Atmospheric Boundary Layer," Journal of Atmospheric Sciences, **46** (11), pp. 1492-1516.

[16] Sorensen, J.N., Mikkelsen, R.F., Henningson, D.S., Ivanell, S., Samast, S., Andersen, S., 2014, "Simulation of Wind Turbine Wakes Using the Actuator Line Technique," Phil Trans., R. Soc. A 373: 20140071. http://dx.doi.org/10.1098/rsta.2014.0071

[17]Lungo, G., Porte-Agel, F., 2014 "Volumetric Scanning of Wind Turbine Wakes Under Convective and Neutral Stability Regimes," Journal of Atmoshperic and Oceanic Technology, **31 (10)**

ANNEX A

ACCRONYMS

ABL	Atmospheric Boundary Layer
CABL	Convective Atmospheric Boundary Layer
CFD	Computation Fluid Dynamics
LES	Large Eddy Simulation
NABL	Neutral Atmospheric Boundary Layer
SOWFA	Simulator for Offshore Wind Farm Applications
TKE	Turbulent Kinetic Energy
WT	Wind Turbine